J Therm Anal Calorim (2011) 105:383–388
DOI 10.1007/s10973-010-1249-z

Thermal behavior of nickel–metal hydride battery during charging at a wide range of ambient temperatures

Kai Zheng Fang · Dao Bin Mu · Shi Chen · Feng Wu · Xiao Jun Zeng

Received: 22 November 2010 / Accepted: 6 December 2010 / Published online: 6 January 2011

Abstract The thermal behavior of D-type Ni–MH battery during charging was investigated at a wide range of ambient temperatures in this work. The temperature measurement of the battery was conducted by using a thermal infrared imager put in a high–low temperature chamber. The ambient temperatures were controlled to −10, 0, 10, 20, 30, and 40 °C during charging. The battery was charged to SOC of 110% in the rate of 1C, 3C, and 5C. Real-time infrared thermal images of battery surface were obtained during charging, as well as temperature change curves. The maximum surface temperature of the battery at the end of charging was stimulated at a higher ambient temperature by curve fitting. It is indicated that the temperature gradient on battery surface will increase with charging rate increase, and the rate of actual temperature rise is almost unrelated to ambient temperature. The simulating result shows that the maximum surface temperature would be over 101 °C if the battery is charged in the rate of 5C under an ambient temperature of 70 °C, which may lead to a safe accident.

Keywords D-type Ni–MH battery · Thermal infrared imager · Ambient temperature · Thermal behavior

Introduction

Ni–MH battery is now widely used in hybrid vehicles and portable electronic devices as a new green secondary battery. The demands of Ni–MH battery have always been at a high level in current market because of its excellent performance such as high energy density, high power density, and long life [1–3]. The fast charging and discharging is needed when the battery is in working, which will cause the battery temperature rise. In particular, fast charging in large current density will result in rapid temperature increasing both on battery surface and inside [4–6]. Although the safety of nickel–metal hydride battery is better than lithium–ion battery [7, 8], the extra high temperature does affect battery performance and even leads to electrolyte leakage, which may bring about explosion hazard [9]. Previous studies have shown that when the maximum temperature on battery surface reached 100 °C, the volume of Ni–MH battery would expand obviously, and the increased internal pressure would break through the safety valve, which gave rise to electrolyte leakage resulting in battery failure. Therefore, the thermal behavior of Ni–MH battery is receiving more attention in recent years, and the simulation of heat generation is also focused in this area. Since Bernardi et al. [10] proposed heat generation rate model, a number of scholars had adopted thermal model to study thermal behavior of battery. Chen et al. [11] established research standards of the thermal behavior of cylindrical lithium ion battery through two-dimensional model. Shi et al. [12] predicted the temperature distribution of Ni–MH batteries by using cylindrical two-dimensional model. However, few works verified the correctness of such conclusions through experiments. Nowadays, many studies are focusing on the thermal behavior of Ni–MH battery during charging, because the thermal behavior during discharging is less obvious. Yang et al. [13, 14] measured the heat generation of Ni–MH battery using quartz calorimeter and obtained the results indirectly from the temperature of

K. Z. Fang · D. B. Mu (✉) · S. Chen · F. Wu · X. J. Zeng
Beijing Key Laboratory of Environmental Science and Engineering, School of Chemical Engineering and Environment, Beijing Institute of Technology, Beijing 100081, China
e-mail: mudb@bit.edu.cn

water. However, it was not available to get the actual heat distribution on battery surface directly. In this article, the thermal behavior of D-type Ni–MH battery in air was studied under different ambient temperatures and real-time monitoring was carried out by using thermal infrared imager, thereby, the heat distribution on battery surface and the temperature change during charging can be observed directly. In addition, the maximum temperature on battery surface at a higher ambient temperature was speculated by simulation method.

Experiment

The testing device used in the experiment is shown in Fig. 1. The heat generation of the battery charged in air can be monitored in real-time through this system.

D-type nickel–metal hydride battery with the capacity of 8Ah was adopted in the experiment. It was cylindrical in stainless steel case with a rated voltage of 1.2 V. In order to ensure the accuracy of tested temperature, the battery surface was painted by matte black in this study. Thus, the emissivity of battery surface can be approximated as 1.

The thermal infrared imager used in the study is VarioCAM hr from German Infra Tec Company. It is a real-time infrared thermal imaging system based on uncooled thermal detector of trace. It can be used at the temperature range from −15 to 50 °C with 0.08 °C thermal sensitivity.

The battery was fixed in a specially designed device for battery charging and discharging, and then it was placed in high–low temperature chamber and connected with an Arbin battery testing instrument. The temperature in the chamber was set to −10, 0, 10, 20, 30, and 40 °C, respectively. The battery was charged to the state of 110% capacity in the rate of 1C, 3C, and 5C under different ambient temperatures. The temperature change on battery surface was recorded by real-time monitoring of the thermal infrared imager.

Results and discussion

The heat distribution can be obtained directly at the end of charging through thermal infrared imaging. Figures 2, 3, and 4 show the heat distribution on battery surface at the

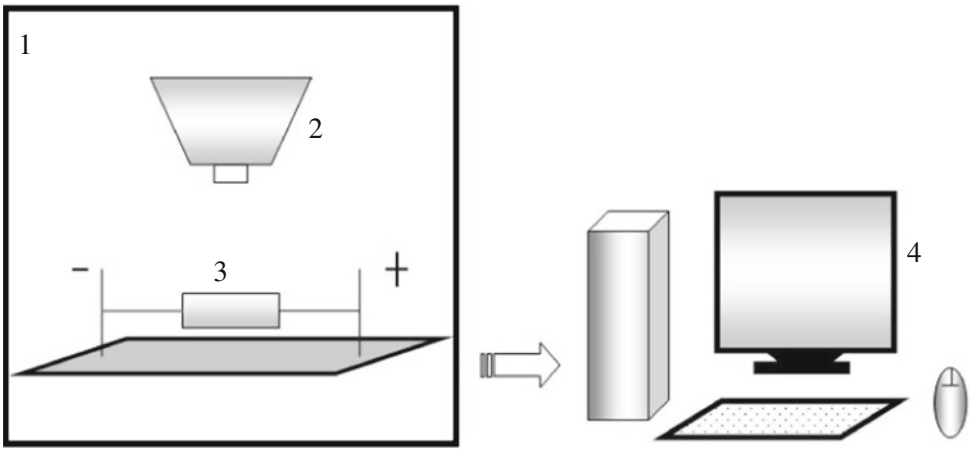

Fig. 1 Experiment equipments. *1* High–low temperature chamber, *2* thermal infrared imager, *3* Ni–MH battery, *4* thermal infrared imaging workstation

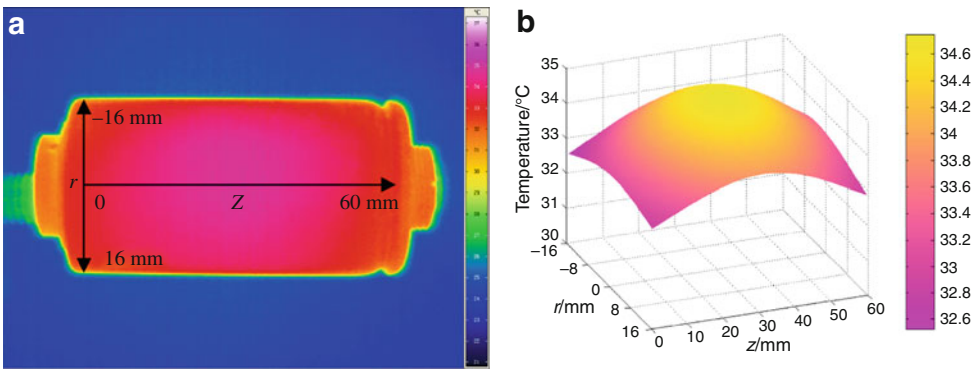

Fig. 2 Battery surface thermal image (**a**) and surface temperature distribution map (**b**) charging of 1C (*z*, *r* stands for axial and radial coordinate, respectively)

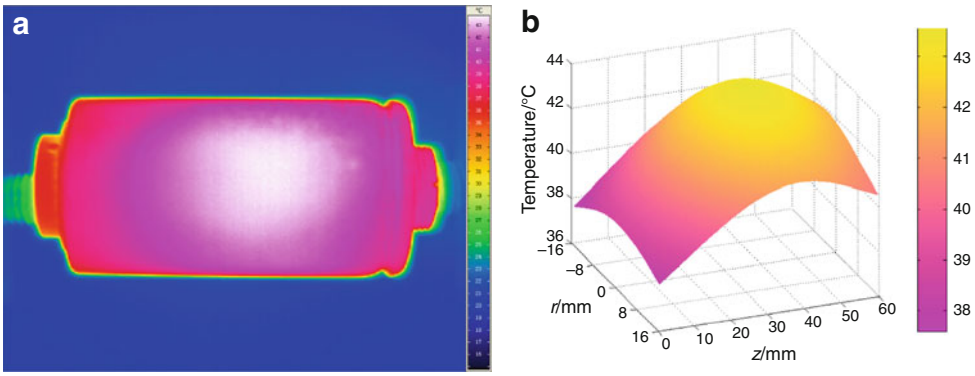

Fig. 3 Battery surface thermal image (**a**) and surface temperature distribution map (**b**) charging of 3C

end of charging with the rate of 1C, 3C, and 5C under the ambient temperature of 20 °C, respectively.

According to Figs. 2, 3, and 4, the differences between the maximum and the minimum temperatures on battery surface are 2.88, 7.02, and 11.30 °C, respectively, at the end of charging in the rate of 1C, 3C, and 5C. The white zones in the thermal images represent the highest temperature area which is closer to the positive region of the battery. The high-temperature region on battery surface gradually enlarges as the charging rate increases. Meanwhile, the temperature gradient in axial direction (z) increases remarkably with charging rate increase. The higher the charging rate, the larger the temperature gradient is. The maximum surface temperature is up to 60.99 °C at the end of charging with the rate of 5C and the highest temperature point corresponding to the coordinate of (r, z) plane locates in (40, 0) on the surface temperature map.

The temperature change curves of the above point when the battery was charged in the rate of 1C, 3C, and 5C at various ambient temperatures are shown in Figs. 5, 6, and 7, respectively.

It is seen that, when the ambient temperature keeps constant, the temperature of battery surface increases with the charging rate increases at the end of charging, while the temperature of the battery charged at 40 °C was higher than those at −10 to 30 °C with the same charging rate. It means that the increased ambient temperature leads to temperature of battery increasing when the charging rate is the same. The temperature of battery charged at −10 °C is lower than the case at 0–40 °C at the end of 1C charging. However, in the cases of 3C and 5C, the temperatures at −10, 0, and 10 °C overlap at the end of curves, which lead to the final temperatures almost the same. The reason for the curves overlapping in Figs. 6 and 7 is that every curve will turn to rise up at some moment, the earlier the curve turn to rise up, the higher the final temperature is. However, with the rise of ambient temperature, the transition time is delayed. Therefore, there is no overlapping of curves when the battery was charged at 30 and 40 °C. The difference of transition time may attribute to the effect of ambient temperature on heat generation during charging. Usually heat generated during charging consists of reaction heat, polarization heat, Ohm heat, and recombination heat [6]. When the battery is charged in high rate, the reaction heat increases as the electrode reaction accelerates; also, the polarization heat increases as the polarization resistance increases; meanwhile Ohm heat increases as the current increases. Therefore, the temperature rise rate of battery is the lowest in the rate of 1C and the highest in 5C. When the battery is at the late stage of charging, hydrogen and oxygen react to generate a lot of heat, so the curves in the

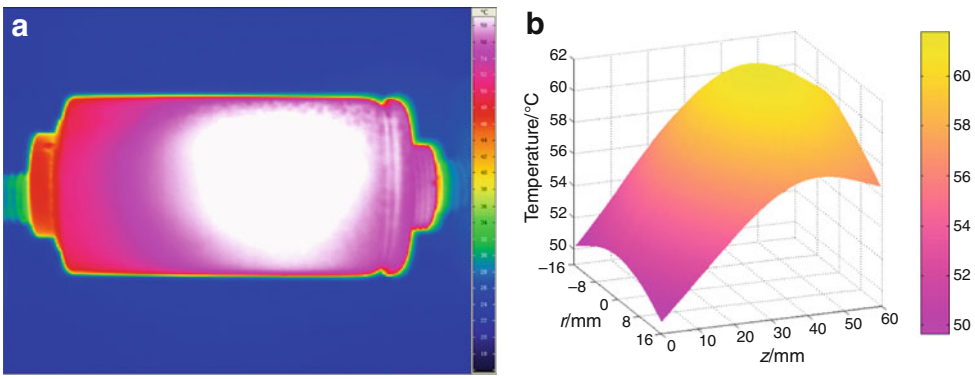

Fig. 4 Battery surface thermal image (**a**) and surface temperature distribution map (**b**) charging of 5C

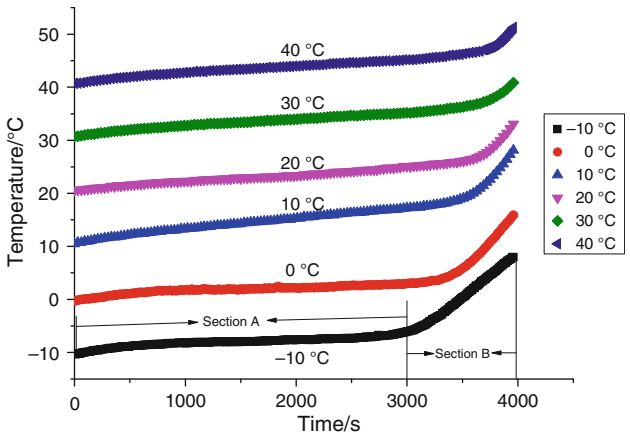

Fig. 5 The temperature change curves of the highest temperature point at various temperatures charging of 1C

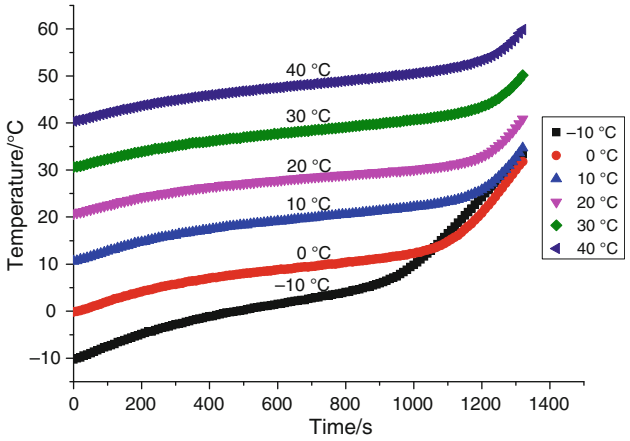

Fig. 6 The temperature change curves of the highest temperature point at various temperatures charging of 3C

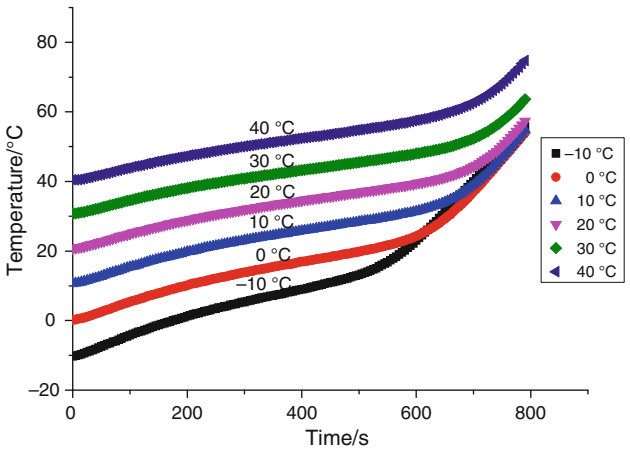

Fig. 7 The temperature change curves of the highest temperature point at various temperatures charging of 5C

figures (Figs. 5, 6, 7) turn to rise up. The transition time is earlier at low temperature and later at high temperature when charged in the same rate under different ambient temperatures. The reason is that hydrogen atoms generate on the surface of alloy at the late stage of charging, theoretically, which will spread internally toward the alloy to form alloy hydride, and this step is decided by the diffusion rate of hydrogen. The diffusion coefficient of hydrogen can be calculated from the equation $D = D_o\exp(-Q/kT)$, where Q is activation energy of atomic diffusion, D_o is diffusion constant, and k is Boltzmann constant. Therefore, it can be found that the rate of diffusion is influenced by the temperature, accordingly, the higher the temperature is, the greater the diffusion coefficient is, and the diffusion rate becomes faster. Therefore, compared with high temperature, the rate of hydrogen diffusion is relatively slow at low temperature, which may cause part of the hydrogen atoms on the alloy surface to aggregate, then the hydrogen will be easy to generate, afterward hydrogen and oxygen react emitting a lot of heat, therefore, the transition time appears earlier than the case at high temperature.

Based on the transition time, the temperature curves under various ambient temperatures can be divided into two sections, namely, the temperature slow-rising stage (section A) and the temperature fast-rising stage (section B) (as marked in Fig. 5). In the transition zone, the central point was taken as the specific transition time, and the temperature rise rates of sections A and B can be acquired through linearly fitting of sections A and B, respectively. Figures 8, 9, and 10 show the temperature rise rate and the transition time curves when charged in the rate of 1C, 3C, and 5C, respectively.

From Figs. 8a, 9a, and 10a, it can be seen that the temperature rise rates of sections A and B increase with the charging rate increasing. The temperature rise rate of section A is far less than section B in the same charging rate. Meanwhile, the distribution of temperature rise rate of section B is more wide. It seems that the rate of actual temperature rise is almost unrelated to ambient temperature. Thus, an average value is assumed the temperature rise rate at higher temperatures. Table 1 shows calculated average rates of temperatures rise in various charging rates.

It is found that the transition time changes with the ambient temperature from Figs. 8b, 9b, and 10b. When charged 1C, 3C, and 5C, the transition time (y) ~ ambient temperature (x) curves are well fitted into exponential function, which are shown in Eqs. 1, 2, and 3.

$$1\text{C} \quad y = 3825.60468 - 458.87545\exp(-0.05893x) \quad -10 \le x \le 40\ ^\circ\text{C} \tag{1}$$

$$3\text{C} \quad y = 1310.47478 - 227.52047\exp(-0.04909x) \quad -10 \le x \le 40\ ^\circ\text{C} \tag{2}$$

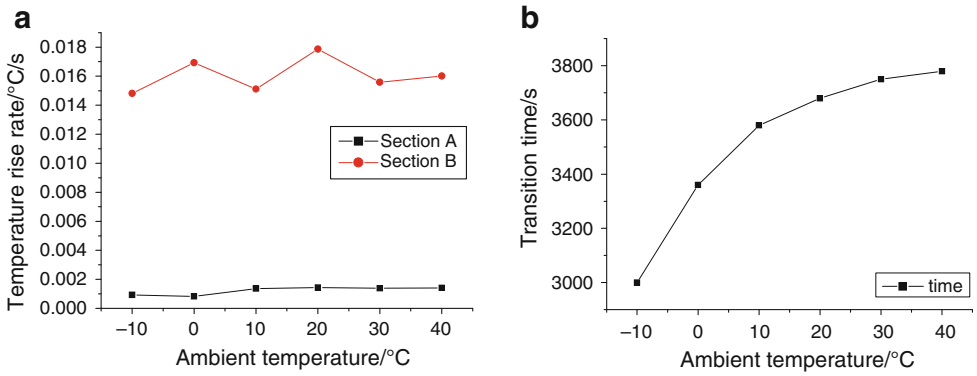

Fig. 8 The temperature rise rate curves (**a**) and the transition time curve (**b**) charging of 1C

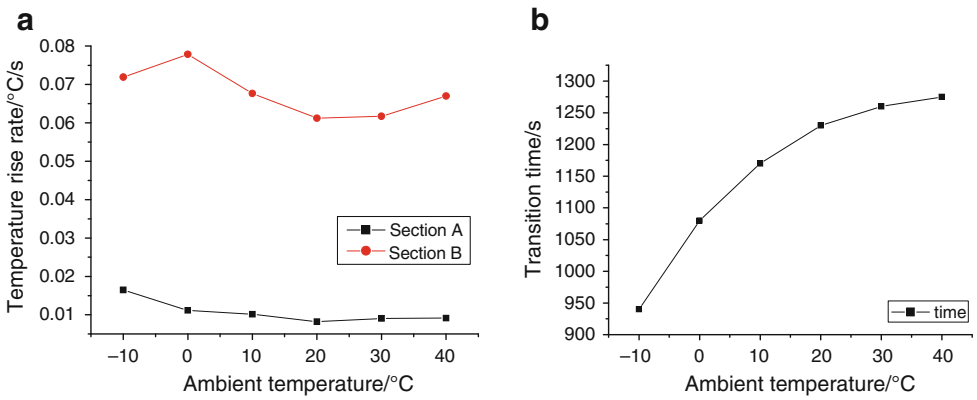

Fig. 9 The temperature rise rate curves (**a**) and the transition time curve (**b**) charging of 3C

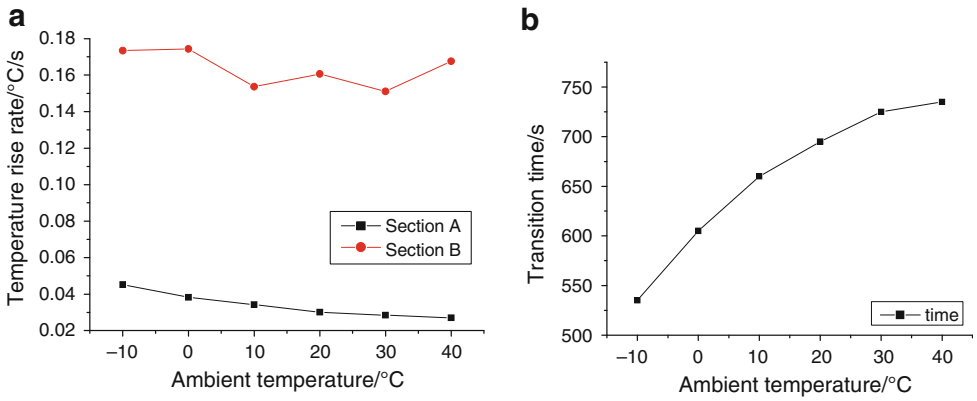

Fig. 10 The temperature rise rate curves (**a**) and the transition time curve (**b**) charging of 5C

Table 1 The average temperature rise rate

	1C/°C s^{-1}	3C/°C s^{-1}	5C/°C s^{-1}
Section A	0.00123	0.01070	0.03390
Section B	0.01610	0.06790	0.16300

$$5\text{C} \quad y = 759.97084 - 143.64233\exp(-0.04503x) \quad -10 \le x \le 40\ ^\circ\text{C} \tag{3}$$

The transition time from section A to section B can be calculated based on exponential functions of (1)–(3). The values at 50, 60, and 70 °C are listed in Table 2, respectively.

The temperature of the highest temperature point on battery surface at the end of charging can also be simulated through this curve fitting. Table 3 gives the simulated temperatures when charged at 50, 60, and 70 °C.

Accordingly, when the ambient temperature reaches 70 °C, the maximum surface temperature will be more than 100 °C under the charging state of 110% capacity in the rate of 5C, which will lead to safety issues. Indeed, the temperature inside the battery pack of electric vehicle may reach 70 °C when it is used at the outdoor temperature over

Table 2 Transition time

	1C/s	3C/s	5C/s
50 °C	3801	1290	745
60 °C	3812	1298	750
70 °C	3818	1303	753

Table 3 Simulated temperature of the highest temperature point at the end of charging

	1C/°C	3C/°C	5C/°C
50 °C	57.25	65.83	82.92
60 °C	67.07	75.38	92.27
70 °C	76.99	85.10	101.89

40 °C in summer. Therefore, in this condition, it is suggested that for safety consideration, high-rate charging should be avoided. And it is better to adopt thermal management system to cool the battery if possible.

Conclusions

(1) Real-time thermal images of Ni–MH battery surface were obtained directly by using infrared thermal imager, by which the highest temperature point on battery surface was determined to study the thermal behavior of the battery during charging.
(2) The temperature gradient on battery surface will get increased as the charging rate increases. The actual temperature rise rate is almost unrelated to ambient temperature when the battery is charged in the same rate. The final temperature of battery is influenced by the transition time.
(3) It is speculated that the highest temperature on battery surface will be more than 100 °C if the battery is overcharged in the rate of 5C at the ambient temperature of 70 °C through simulating calculation, which may be very dangerous.

Acknowledgment This work is supported by National 973 Program of China (Grant No. 2009CB220100).

References

1. Wu MS, Wang YY, Wan CC. Thermal behavior of nickel/metal hydride battery during charge and discharge. J Power Sources. 1998;74:202–10.
2. Zhang ZL, Zhong MH, Liu FM, et al. In situ study of charge and discharge of Ni–MH battery using the combined method of electrochemistry and microcalorimetry. J Therm Anal Calorim. 1999;58:413–9.
3. Harmel J, Ohms D. Investigation of the heat balance of bipolar Ni/MH-batteries. J Power Sources. 2006;155:88–93.
4. Ohms D, Kohlhase M, Benczúr-Ürmössy G, et al. High performance nickel–metal hydride battery in bipolar stack design. J Power Sources. 2002;105:120–6.
5. Wu MS, Hung YH, Wang YY, et al. Heat dissipation behavior of the nickel/metal hydride battery. J Electrochem Soc. 2000; 147:930–5.
6. Sato N, Yagi K. Thermal behavior analysis of nickel metal hydride batteries for electric vehicles. JSAE Rev. 2000;21: 205–11.
7. Onda K, Ohshima T, Nakayama M. Thermal behavior of small lithium-ion battery during rapid charge and discharge cycles. J Power Sources. 2006;158:535–42.
8. Yang K, An JJ, Chen S. Temperature characterization analysis of LiFePO4/C power battery during charging and discharging. J Therm Anal Calorim. 2010;99:515–21.
9. Ying T, Gao X, Hu W, et al. Studies on rechargeable Ni/MH batteries. Int J Hydrog Energy. 2006;31:525–30.
10. Bernadi D, Pawlikowski E, Newman J. A general energy balance for battery systems. J Electrochem Soc. 1985;132:5–12.
11. Chen SC, Wang YY, Wan CC. Thermal analysis of spirally wound lithium batteries. J Electrochem Soc. 2006;153:A637–48.
12. Shi JZ, Wu F, Chen S, et al. Thermal analysis of rapid charging nickel/metal hydride batteries. J Power Sources. 2006;157:592–9.
13. Yang K, Li DH, Chen S, et al. Thermal behavior of nickel/metal hydride battery during charging and discharging. J Therm Anal Calorim. 2009;2:455–9.
14. Yang K, An JJ, Chen S. Influence of additives on the thermal behavior of nickel/metal hydride battery. J Therm Anal Calorim. 2010;102:953–9.